

High-Temperature Superconductivity in Alkaline and Rare Earth Polyhydrides at High Pressure: A Theoretical Perspective

Eva Zurek^{1, a)} and Tiange Bi¹

Department of Chemistry, State University of New York at Buffalo, Buffalo, NY 14260-3000, USA

The theoretical exploration of the phase diagrams of binary hydrides under pressure using *ab initio* crystal structure prediction techniques coupled with first-principles calculations has led to the *in silico* discovery of numerous novel superconducting materials. This Perspective article focuses on the alkaline earth and rare earth polyhydrides whose superconducting critical temperature, T_c , was predicted to be above the boiling point of liquid nitrogen. After providing a brief overview of the computational protocol used to predict the structures of stable and metastable hydrides under pressure, we outline the equations that can be employed to estimate T_c . The systems with a high T_c can be classified according to the motifs found in their hydrogenic lattices. The highest T_c s are found for cages that are reminiscent of clathrates, and the lowest for systems that contain atomic and molecular hydrogen. A wide variety of hydrogenic motifs including 1- and 2-dimensional lattices, as well as $H_{10}^{\delta-}$ molecular units comprised of fused $H_5^{\delta-}$ pentagons are present in phases with intermediate T_c s. Some of these phases are predicted to be superconducting at room temperature. Some may have recently been synthesized in diamond anvil cells.

I. INTRODUCTION

The pressure induced metallization of hydrogen was first proposed by J. D. Bernal, but only later reported in the literature by Wigner and Huntington, who predicted that at $P > 25$ GPa hydrogen would become an alkali metal-like monoatomic solid¹. It turned out that this was a gross underestimate: the lightest element has stubbornly resisted metallization up to center of the Earth pressures in a diamond anvil cell (DAC)^{2–10}. A few recent studies have presented evidence indicative of metallization^{11,12}, but the interpretation of the experimental results has been questioned^{13–15}.

Why has blood, sweat and tears gone into attempts to metallize hydrogen? And what makes metallic hydrogen so special that it has been dubbed *the holy grail of high pressure research*? The reason can be traced back to Ashcroft, who predicted that the large phonon frequencies (a result of the small mass of H), large electron phonon coupling (arising from the strong covalent bonds between the H atoms, and lack of core electrons), wide bands, and substantial density of states (DOS) at the Fermi level (E_F) would render this elusive substance superconducting at high temperatures¹⁶. Indeed, first principles calculations have estimated high values for the superconducting critical temperature (T_c): 242 K at 450 GPa in the molecular phase¹⁷, and as high as 764 K for monoatomic hydrogen near 2 TPa¹⁸. Thus, one way to make superconducting metallic hydrogen is by achieving the appropriate T/P conditions.

However, *chemistry* may be able to hasten the metallization of hydrogen. In a seminal manuscript Ashcroft pointed out that because the hydrogen in solids comprised of the group 14 hydrides is “chemically precompressed”, they may become metallic at lower pressures than elemental hydrogen^{19,20}. In other words, hydrogen’s interaction with the tetragen atoms would modify the H-H distances and densities in such a way that less external physical pressure would be required

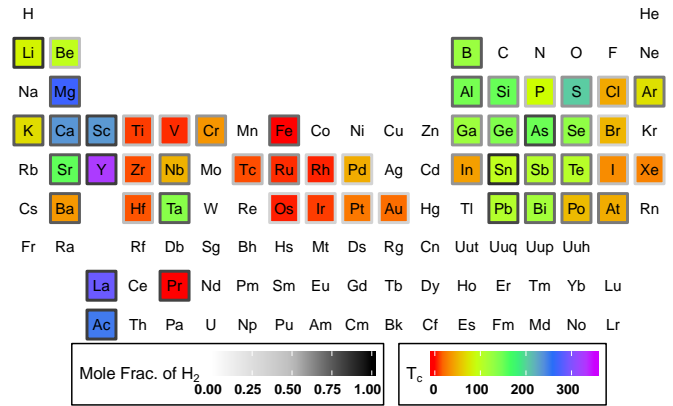


FIG. 1. The periodic table colored according to the highest T_c value theoretically predicted for a binary hydride containing the given element⁵³. The coloring scheme, in Kelvin, is given below. The H_2 mole fraction in the hydride with the highest T_c is represented by the color outlining the element. It ranges from white (low) to black (high). If the element is not enclosed in a colored box, then theoretical predictions of the T_c s of its hydrides are not available. Typically this is because the phases predicted to be stable are not metallic or are poor metals, and they are therefore unlikely to have a high T_c .

to achieve a metallic state. Moreover, Ashcroft hypothesized that these compressed hydrides would have the same properties conducive towards high temperature superconductivity as hydrogen itself, thereby suggesting a parallel route to metallizing hydrogen. These predictions led to a plethora of theoretical, and a few experimental studies that searched for superconductivity in hydrides known to exist at 1 atm, including SiH_4 ^{21–31}, GeH_4 ^{32–36}, and AlH_3 ^{37–40}. But, because pressure is known to affect the chemical compositions that are stable^{41–43}, systems with stoichiometries that are not observed at 1 atm, e.g. $SiH_4(H_2)_n$, $n > 0$,^{44–50} and LiH_n , $n > 1$,^{51,52} were also investigated. The possibility of accessing novel combinations and electronic structures under pressure dramatically widens the phase space wherein a high temperature superconductor

^{a)}Electronic mail: ezurek@buffalo.edu

can be found.

High pressure experiments can be very costly, and the results can be difficult to analyze. It is therefore no surprise that the dramatic improvement of computer hardware, coupled with the development of robust methods for *a priori* crystal structure prediction (CSP) using Density Functional Theory (DFT) calculations has led to the rapid *in silico* exploration of the phase diagrams of materials under pressure. Many investigations have focused on the parallel route of metallizing hydrogen inspired by Ashcroft's predictions^{19,20}. In just over a decade the phase diagrams of most binary hydrides under pressure have been calculated⁵⁴⁻⁶³. T_c s that approach, and even surpass, room temperature have been calculated for a number of phases that are predicted to be stable at pressures attainable in DACs.

The periodic table illustrated in Fig. 1 graphically shows the highest undisputed⁶⁴ T_c s predicted for each element's polyhydride⁵³. Two regions contain hydrides that are the most promising for high temperature superconductivity: (i) many of the *p*-block elements in groups 13-16, and (ii) a subset of the alkaline earth and rare earth metals. High temperature superconductivity was found within the first region when a T_c of 203 K near 150 GPa was measured in a sample of compressed hydrogen sulfide⁶⁵. Not only does this material possess the highest confirmed T_c to date, remarkably it is also a Bardeen-Cooper-Schrieffer (BCS) type superconductor⁶⁶. As described in more detail elsewhere⁶¹, this discovery was not serendipitous; theoretical investigations inspired⁶⁷ experiment and helped to interpret the results⁶⁸. Superconductivity in the sulphur/hydrogen system under pressure has been the topic of numerous studies⁶⁹⁻¹⁰⁰, and it has been reviewed^{61,101,102}.

This Perspective focuses on studies of hydrides in the second region, the alkaline and rare earths, whose predicted T_c s are at least as high as the boiling point of liquid nitrogen. Recent experiments tantalize with the promise of room temperature superconductivity in these systems, with measured T_c s as high as 215 K¹⁰³ or 260-280 K¹⁰⁴ in the lanthanum/hydrogen system under pressure. Sec. II provides a brief overview of the computational approaches used for the *ab initio* prediction of the structures of novel pressure stabilized hydrides, and Sec. III discusses the equations used to approximate T_c . The predicted structures and their superconducting properties are discussed in Sec. IV, which is organized by the motifs found in these phases' hydrogenic lattices: clathrate-like arrangements, mixed atomic and molecular hydrogen, and other unique discrete or periodic hydrogenic motifs, such as $H_5^{\delta-}$ "pentagons" or 2-dimensional sheets. A brief outlook is provided in Sec. V.

II. COMPUTATIONAL AND THEORETICAL CONSIDERATIONS

Pressure can have a profound effect on the compositions, structures, properties and stability of solid phases^{41-43,105-113}. Who would have guessed that the "simple metal" sodium becomes an insulator by 200 GPa¹¹⁴, the "noble" gas helium reacts with sodium to form a stable Na_2He ^{115,116} phase at

113 GPa, and hydrides with unusual stoichiometries such as NaH_3 ¹¹⁷, $Xe(H_2)_8$ ¹¹⁸ and FeH_5 ¹¹⁹ can be synthesized in a DAC? Such chemistry could not have been predicted using rules and bonding schemes that are based upon our experience at 1 atm. At the same time, experiments that approach the pressures in the Earth's core (~ 350 GPa) are challenging, and the results can be difficult to analyze. This has led to the development of a symbiotic relationship between theoreticians and experimentalists, where a feedback loop between experiment and theory has often led to important discoveries.

Because of the difficulty inherent in performing high pressure syntheses and fully characterizing the phases made, many theoretical groups have employed *a priori* methods for crystal structure prediction (CSP) to propose stable candidate structures. Structure prediction is a global optimization problem, where the goal is to determine the unit cell parameters, and atomic coordinates that correspond to the global minimum, as well as low lying local minima, in the potential energy surface (PES). However, as with all optimization problems, it is not possible to guarantee that the global minimum has been found within a CSP search. Thus, many of the algorithms that have been adapted towards CSP employ well known metaheuristics that can find sufficiently good solutions for the minima. This includes: (quasi) random searches, techniques based on swarm behavior, evolutionary (genetic) algorithms, basin or minima hopping, as well as simulated annealing and metadynamics. A number of excellent reviews describing these methods¹²⁰⁻¹³⁰, and the synergy between CSP and experiment in high pressure research^{41,56,60,123,124} are available.

Typically hundreds, if not thousands, of structures are optimized to the nearest local minimum within a single CSP search. Moreover, often multiple searches need to be carried out for different stoichiometries and for a range of pressures. Because computations of the vibrational contributions to the free energy are significantly more time consuming than geometry optimizations, most CSP searches explore the 0 K PES. Reliable force fields are often not available for matter at extreme conditions, so the local optimizations are usually performed using DFT with a functional based on the generalized gradient approximation (GGA); often the Perdew, Burke and Enzerhof (PBE)¹³¹ GGA is employed. Hybrid functionals such as HSE06¹³² or PBE0¹³³ have so far not been used during CSP because of the immense computational expense involved. However, the inclusion of Hartree-Fock exchange can significantly affect the calculated transition pressures between different phases,¹³⁴⁻¹³⁶ stabilization pressures¹³⁷⁻¹³⁹, computed T_c values¹⁴⁰, and it can lead to symmetry breaking structural (Peierls) distortions¹⁴¹. Even though still rare, it is becoming more common to reoptimize the most stable structures found in a GGA-CSP search using hybrid functionals¹³⁷⁻¹³⁹. In situations where metallization occurs because of pressure induced band broadening of the valence and conduction bands, and their eventual overlap, GGA functionals predict a too low metallization pressure. Hybrid functionals provide better estimates of the pressure at which band gap closure occurs. The inclusion of dispersion can also affect transition pressures for molecular solids^{142,143}, and DFT+U has been employed for strongly correlated systems¹⁴⁴. An *adaptive* genetic algo-

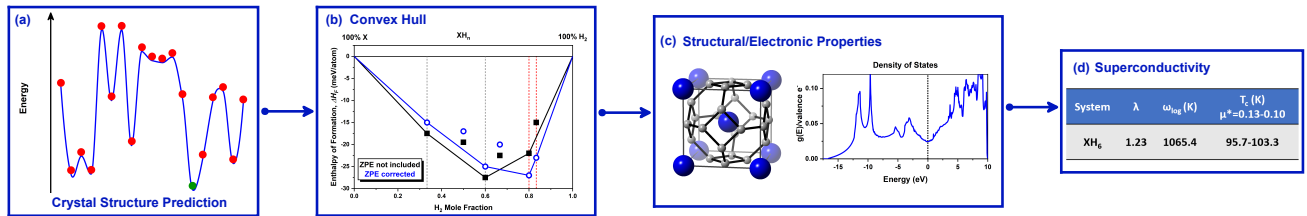


FIG. 2. Typical workflow used to predict pressure stabilized hydride based superconductors. (a) Candidate structures are found using *ab initio* crystal structure prediction techniques. (b) The ΔH_F of the most promising phases are plotted vs. the mole fraction of H_2 they contain. The convex hulls without, and with ZPE contributions are determined. (c) The electronic structure of thermodynamically stable and select metastable species are computed to identify systems that have a high DOS at E_F . (d) Electron phonon coupling calculations are carried out, and the results are used to estimate T_c via the equations given in Sec. III.

rithm, which uses DFT calculations performed on a small set of candidate structures to parametrize, on-the-fly, classical potentials that are then employed for the local minimizations has successfully been applied to predict the structures of binary and ternary phases under pressure¹⁴⁵.

For systems containing light elements the inclusion of the zero point energy (ZPE) can influence the relative enthalpies of different phases, as well as the identity of the thermodynamically stable species and their stability ranges. This is especially true if the hydrogenic sublattices of the structures whose enthalpies are compared have different motifs. Cold melting, which can occur if the difference in enthalpy between different phases is smaller than the ZPE, has been proposed for metal hydrides that contain a heavy element^{146,147}. It is currently standard practice to consider how the ZPE affects the stability of the phases found in a CSP search carried out at 0 K, but finite temperature contributions to the free energy are rarely considered, even though they may also be important (as it has been shown for elemental hydrogen¹⁴⁸). Because the experimental conditions employed can affect which phases (i.e. stable or metastable) are made^{149,150}, it is important for theory to identify not only the global minimum, but also low lying local minima¹⁵¹.

Fig. 2 illustrates the typical workflow employed by theoreticians searching for novel pressure-stabilized superconducting phases, including those discussed in this Perspective. First, CSP searches are carried out on the 0 K GGA PES as a function of composition and pressure. Promising candidate structures are optimized using more accurate settings, and their enthalpies of formation, ΔH_F , are plotted vs. the mole fraction of H_2 they contain. The ΔH_F are employed to generate the convex hull, which is the set of line segments below which no other points lie. The phases whose ΔH_F comprise the hull are thermodynamically stable. Phonon calculations are carried out to confirm dynamic stability of phases that are on the hull or close to it, and the results are used to construct a new convex hull that includes the ZPE contributions to the enthalpy at 0 K. The structure, and electronic structure of select systems are computed and analyzed. In the following Section we described the methods employed to estimate the T_c of the most promising structures.

All of the phases discussed in the following sections were predicted using particle swarm optimization^{152,153}, evolutionary

algorithms^{154,155} or *ab initio* random structure searching¹⁵⁶. Because they did not become metallic because of pressure induced band broadening, it was not necessary to recompute their DOS' with a hybrid functional. Even though it is possible that geometry optimization with a hybrid functional would result in a Peierls distortion that opens up a band gap, this was not considered. Because of the high computational cost associated with performing electron phonon coupling calculations, T_c was estimated using GGA calculations within the harmonic approximation.

III. ESTIMATING THE SUPERCONDUCTING CRITICAL TEMPERATURE

In this section the equations that are typically employed to estimate T_c for compressed hydrides from first principles calculations are introduced. In the past these techniques have been successfully applied to a wide range of metallic systems¹⁵⁷. If the superconducting properties of a material can be described using BCS theory, or its extensions, the material is referred to as a conventional superconductor. The electron phonon coupling mechanism that leads to superconductivity within BCS theory can be pictured as follows. When an electron passes through a crystalline lattice of positively charged ions, the Coulomb attraction between the electron and the ion causes the lattice to distort. The ionic displacement, in turn, attracts another electron with opposite spin and momentum. The two electrons become correlated and form a boson-like quasiparticle called a Cooper pair. All of the Cooper pairs in a superconductor break up at a temperature higher than T_c , thereby destroying the superconducting state.

Within BCS theory, T_c can be estimated via

$$T_c = 1.14 \langle \omega \rangle \exp \left[\frac{-1}{g(E_F)V} \right] \quad (1)$$

where $\langle \omega \rangle$ is the average phonon energy, $g(E_F)$ is the single spin electronic DOS at E_F , and V is the pairing potential between two electrons that occurs via the electron phonon interaction (which is assumed to be constant within $2\hbar\omega_{\text{cut}}$ of the Fermi surface, and zero otherwise)^{158,159}. The cutoff frequency, ω_{cut} , is often taken to be the Debye frequency or the

average frequency, and it defines the size of the superconducting band gap.

Despite the tremendous successes of BCS theory in describing the properties of conventional superconductors, substantial differences between theory and experiment became apparent, for example for the metals Pb and Hg. The reason for this turned out to be that the assumption of constant V is too simple: the electron phonon interaction is not instantaneous, but rather it is retarded in time, and the quasiparticle states have a finite lifetime. Eliashberg theory is an extension of BCS theory that explicitly includes the retardation effects¹⁶⁰. It is beyond the scope of this Perspective to discuss the Eliashberg equations, which can be solved numerically. However, we introduce the key quantity of Eliashberg theory, the Eliashberg spectral function, which can be calculated (from first principles) or measured (by inverting tunnelling spectra).

The Eliashberg spectral function, $\alpha^2 F(\omega)$, is defined as:

$$\alpha^2 F(\omega) = \frac{1}{2\pi g(E_F)} \sum_{qj} \frac{\gamma_{qj}}{\omega_{qj}} \delta(\hbar\omega - \hbar\omega_{qj}), \quad (2)$$

where the linewidth, γ_{qj} , of a phonon mode j with a wave-vector q , ω_{qj} , is given by:

$$\gamma_{qj} = 2\pi\omega_{qj} \sum_{knm} |g_{kn,k+qm}^j|^2 \delta(\epsilon_{kn} - E_F) \delta(\epsilon_{k+qm} - E_F). \quad (3)$$

These equations describe the scattering of an electron on the Fermi surface with a resulting transfer of momentum to a phonon, where $g_{kn,k+qm}^j$ is the electron phonon matrix element, or the probability, associated with this process. Given the Eliashberg function, the electron phonon coupling, λ , can be calculated via:

$$\lambda = 2 \int_0^\infty \frac{\alpha^2 F(\omega)}{\omega} d\omega. \quad (4)$$

The Eliashberg formalism requires as input a parameter that describes the screened Coulomb repulsion between the electrons within a Cooper pair. This renormalized Coulomb repulsion parameter, μ^* , is often called the Coulomb pseudopotential. Analytical expressions that can be used to approximate μ^* have been proposed, but typically it is used as a free parameter with reasonable values lying in the range of 0.1-0.2. We note that there is one theoretical approach, density functional theory for superconductors (SCDFT), which takes into account the retardation effects, and does not require any empirical parameters for the calculation of T_c ^{161,162}. However, only a few studies have used SCDFT for hydrides under high pressure, for example Refs.^{74,163}.

One of the first simple expressions that could be used to estimate T_c was developed by McMillan. Based on twenty-two numerical solutions of the Eliashberg equations for $0 \leq \mu^* < 0.25$, $0 < \lambda < 1.5$, and a single shape for the $\alpha^2 F(\omega)$ function modeled after the phonon DOS in Nb, McMillan showed that the following expression, where Θ_D is the Debye temperature, could be used to provide a reasonable estimate for T_c .¹⁶⁴

$$T_c = \frac{\Theta_D}{1.45} \exp \left[-\frac{1.04(1 + \lambda)}{\lambda - \mu^*(1 + 0.62\lambda)} \right]. \quad (5)$$

Subsequently, Allen and Dynes carried out 200 numerical solutions for various shapes of the Eliashberg function, using a wide range of λ values^{165,166}. They proposed the following modification of the McMillan equation:

$$T_c = \frac{\omega_{\text{ln}}}{1.2} \exp \left[-\frac{1.04(1 + \lambda)}{\lambda - \mu^*(1 + 0.62\lambda)} \right], \quad (6)$$

where ω_{ln} is the logarithmic average frequency of the phonon modes obtained via

$$\omega_{\text{ln}} = \exp \left[\frac{2}{\lambda} \int_0^\infty \frac{d\omega}{\omega} \alpha^2 F(\omega) \ln \omega \right]. \quad (7)$$

Usually, once DFT calculations have been carried out to determine the Eliashberg spectral function, and from it λ , T_c is estimated via Eq. 6 for a range of μ^* values. However, whereas the Allen-Dynes modified McMillan equation implies that T_c reaches a maximum limit when $\lambda \rightarrow \infty$, a maximum does not exist for the exact solution of the Eliashberg equations. In cases where the electron phonon coupling is strong, i.e. $\lambda \gtrsim 1.5$, Eq. 6 often yields a lower limit to T_c . To remedy this, Allen and Dynes proposed multiplying Eq. 6 by scaling factors that correct for the strong coupling, and shape dependence of T_c ¹⁶⁵. However, for the studies discussed herein, T_c was typically estimated solving the Eliashberg equations when λ was large.

IV. HYDROGENIC MOTIFS

A. Clathrate Based Hydrogenic Lattices

A number of CSP-based studies have computed very high T_c s for binary alkaline earth or rare earth metal hydrides whose hydrogenic lattices are reminiscent of clathrates. The first system of this type to be predicted was a CaH₆ phase, which was thermodynamically and dynamically stable above 150 GPa¹⁶⁷. The building block of this phase is the H₂₄ sodalite-like cage illustrated in the top panel of Fig. 3(a), which consists of six square and eight hexagonal faces. The metal atom lies in the center of this cage, and because the shortest H-H distance measures 1.24 Å, these hydrogen atoms are only weakly bonded to each other. The crystalline lattice that is formed from joining the [4⁶6⁸] polyhedra at the faces, shown in the bottom panel of Fig. 3(a), has $Im\bar{3}m$ symmetry. The band structure of $Im\bar{3}m$ CaH₆ contains degenerate bands at the Γ point that are partially occupied. Therefore, Wang et al. suggested that a Jahn-Teller distortion, which removes this degeneracy, could yield a substantial electron phonon coupling parameter. Indeed, this phase was calculated to have a remarkably large λ of 2.69, with the most significant contribution arising from modes associated with the vibrations of the atoms comprising the H₄ faces. Because of the large λ , T_c was estimated by solving the Eliashberg equations. It was calculated to be between 220-235 K for typical values of μ^* , as shown in Table I, and it decreased at higher pressures.

The prediction of high T_c in CaH₆ inspired a computational study of an isotypic MgH₆ phase, which was found to become stable with respect to decomposition into MgH₂ and H₂

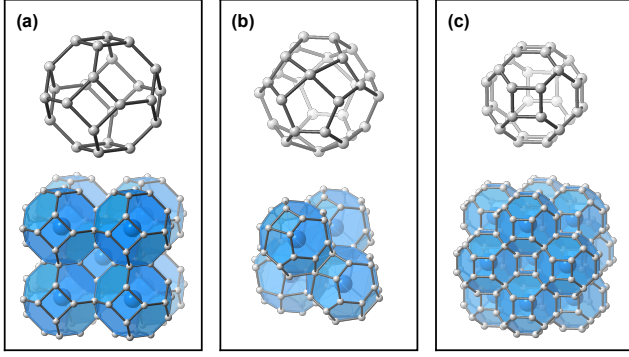


FIG. 3. (Top panel) The hydrogenic clathrate cage structures, and (bottom panel) extended: (a) $Im\bar{3}m$ MH_6 , (b) $P6_3/mmc$ MH_9 and (c) $Fm\bar{3}m$ MH_{10} systems they form with a subset of the alkaline earth and rare earth metals (see Table I). White balls represent the hydrogen atoms, and the metal atoms are faint blue.

above 263 GPa when the ZPE was included¹⁶⁸. But, because a convex hull plotting the ΔH_F of $Im\bar{3}m$ MgH_6 along with the ΔH_F of other stoichiometries that were previously found to be stable at lower pressures¹⁷⁷ was not constructed, it is not clear if MgH_6 is thermodynamically stable or if it is only metastable. The estimated T_c of MgH_6 at 300 K, see Table I, was somewhat higher than the largest T_c calculated for CaH_6 . An isotopic strontium hexahydride was not a local minimum on the PES. However, $R\bar{3}m$ SrH_6 , which can be derived from the $Im\bar{3}m$ structure by elongating four out of six of the closest metal-metal contacts and distorting the face that bisects them so it is no longer hexagonal, was stable at ~ 250 GPa^{178,179}. This symmetry breaking distortion transformed the sodalite hydrogenic lattice into one-dimensional helical chains, and the resulting structure had a smaller λ , and concomitantly a lower T_c ⁶² than its lighter cousins. A structurally analogous BaH_6 phase with a high T_c could not be located via CSP¹⁸⁰.

Moving to the d -block elements, computations have shown that ScH_6 ^{169-171,181} and YH_6 ^{171,172,174} phases with $Im\bar{3}m$ symmetry are also stable at pressures attainable in DACs. A related $I4/mmm$ symmetry ZrH_6 phase, which can be obtained via a distortion of the $Im\bar{3}m$ lattice, has also recently been found via CSP calculations¹⁷³. In one study¹⁷¹ $Im\bar{3}m$ LaH_6 was computed to be thermodynamically stable at 100 GPa and 150 GPa, whereas in another investigation¹⁷⁴ the LaH_6 stoichiometry was predicted to lie slightly above the convex hull, and assume the same $R\bar{3}m$ symmetry structure previously found for SrH_6 . As shown in Table I, the electron phonon coupling of YH_6 was computed to be particularly high, $\lambda = 2.93$, and therefore its T_c was estimated to be at least 100 K higher than any of the other stable superconducting d -block hexahydrides.

The $[4^65^66^6]$ H_{29} polyhedron shown in the top panel of Fig. 3(b) is comprised of six irregular squares, six pentagons and six hexagons. It is the building block of a hydrogenic clathrate-like lattice with $P6_3/mmc$ symmetry that has

TABLE I. Electron phonon coupling parameter, λ , and superconducting critical temperature, T_c , of phases assuming the $Im\bar{3}m$ (MH_6), $P6_3/mmc$ (MH_9) and $Fm\bar{3}m$ (MH_{10}) sodalite structures illustrated in Fig. 3 computed at the pressures, P , and using the values of the Coulomb pseudopotential, μ^* , listed. Data is also provided for three structurally related phases that can be derived via a symmetry breaking distortion of the clathrate cages.

System	P (GPa)	λ	μ^*	T_c (K)
MgH_6	300	3.29	0.12	263 ^{a,168}
CaH_6	150	2.69	0.13-0.10	220-235 ^{b,167}
SrH_6^*	250	1.10	0.10	156 ^{b,62}
ScH_6	350	1.25	0.10	135 ^{a,169} , 169 ^{b,169}
ScH_6	285	1.33	0.13-0.10	130-147 ^{a,170}
ScH_6^\dagger	300	1.20	0.13-0.10	90-100 ^{b,c,171}
YH_6	120	2.93	0.13-0.10	251-264 ^{b,171,172}
ZrH_6^\ddagger	295	1.20	0.13	114 ^{b,173}
LaH_6	100	2.00	0.13-0.10	150-160 ^{b,c,171}
ScH_9	400	1.50	0.13-0.10	150-190 ^{b,c,171}
YH_9^\ddagger	150	4.42	0.13-0.10	276-253 ^{b,171}
YH_{10}	400	2.41	0.13-0.10	287-303 ^{b,171}
YH_{10}	250	2.58	0.13-0.10	244-265 ^{a,174} , 305-326 ^{b,174}
LaH_{10}^\ddagger	200	2.28	0.10	288 ^{a,171}
LaH_{10}	210	3.41	0.13-0.10	219-238 ^{a,174} , 274-286 ^{b,174}
LaH_{10}^\ddagger	200	3.57	0.13-0.10	218-200 ^{a,175} , 245-229 ^{b,175}
AcH_{10}^\S	200	3.46	0.15-0.10	177-204.1 ^{a,176} , 226-251 ^{b,176}

^a T_c was calculated using the Allen-Dynes modified McMillan equation, Eq. 6.

^b T_c was calculated by solving the Eliashberg equations numerically.

^c Values were estimated from plots in the original papers.

* This $R\bar{3}m$ symmetry phase can be derived by distorting the $Im\bar{3}m$ structure.

† At this pressure the enthalpy of a different phase was slightly lower than for the clathrate structure whose T_c is provided.

‡ This $I4/mmm$ symmetry phase can be derived by distorting the $Im\bar{3}m$ structure.

§ This stoichiometry did not lie on the convex hull without ZPE at 0 K.

‡ This $C2/m$ symmetry phase can be derived by distorting the $Fm\bar{3}m$ structure.

§ This $R\bar{3}m$ symmetry phase can be derived by distorting the $Fm\bar{3}m$ structure.

been predicted for a number of MH_9 stoichiometry rare-earth hydrides¹⁷¹. Phases with the MH_{10} stoichiometry, on the other hand, were often found to assume an $Fm\bar{3}m$ symmetry structure comprised of the H_{32} $[4^66^{12}]$ polyhedron, which is shown in Fig. 3(c)^{171,174}. In the clathrate and zeolite community the latter is known as ‘AST’¹⁸². The stability of the clathrate cages under pressure was attributed to their dense packing, which yields a substantially lower PV term to the enthalpy. For example, at 300 GPa a $P6_3/mmc$ symmetry YH_9 clathrate phase had the smallest volume out of any of the 500 lowest enthalpy structures found via CSP searches¹⁷¹. In some cases the enthalpy of a phase that did not possess a clathrate-like structure was slightly lower, but the ZPE-corrected enthalpies of the two dynamically stable phases were within a few meV/atom of each other¹⁷¹. However, because the estimated T_c s of the clathrate-like structures were significantly

higher, they are provided in Table I. Below 210 GPa, $Fm\bar{3}m$ LaH_{10} was not a minimum on the PES, but a $C2/m$ symmetry lattice that could be derived from the ideal structure via a slight distortion was dynamically stable¹⁷⁵.

As shown in Table I, enticingly high T_c values, some of which even surpass room temperature, have been computed for the YH_9 , YH_{10} and LaH_{10} stoichiometries. Although stable clathritic LaH_9 , CeH_9 , CeH_{10} , and PrH_9 phases were also found via CSP, their computed T_c values were much lower, $< 56 \text{ K}$ ¹⁷¹, because the lower frequency vibrations, which are a result of the heavier element, reduce T_c in a BCS superconductor. On the other hand, a metastable $R\bar{3}m$ symmetry AcH_{10} phase was computed to have a quite high T_c ¹⁷⁶. Its hydrogenic lattice resembled the clathrate structure illustrated in Fig. 3(c), except the square faces were replaced by trapezoids. Out of any of the binary hydrides studied computationally YH_9 , YH_{10} and LaH_{10} hold the record T_c values to date, as seen in Fig. 1.

The aforementioned theoretical predictions inspired experimental studies. Last year a superhydride of lanthanum consistent with the theoretically predicted structure for LaH_{10} was synthesized at 170 GPa, and decompression led to a $Fm\bar{3}m \rightarrow R\bar{3}m \rightarrow C2/m$ phase transformation¹⁸³. And, two very recent studies observed dramatic drops in resistivity in the lanthanum/hydrogen system under pressure, tantalizing with the allure of high temperature superconductivity^{103,104}. If confirmed, both of these findings would break the current record for the highest measured T_c values previously observed in the hydrogen/sulfur system⁶⁵. Somayzulu et al. measured a T_c of between 245-280 K at 190-200 GPa in a sample whose diffraction peaks were consistent with the previously synthesized $\text{LaH}_{10\pm x}$ phase¹⁰⁴. As Table I reveals, this value is in good agreement with theoretical estimates for both the $Fm\bar{3}m$ and the $C2/m$ symmetry LaH_{10} phases. Drozdov and co-workers, who employed a different experimental technique to synthesize a so-far uncharacterized superhydride of lanthanum, reported a maximum T_c of 215 K at 150 GPa¹⁰³. Because the samples were synthesized using different methods, and the measurements were obtained at different pressures it is likely that the phase, or mixture of phases, made in the two studies are not the same.

B. Mixed Molecular and Atomic Hydrogen

Many of the alkali metal, alkaline earth and rare earth polyhydrides that are stable under pressure possess both atomic and molecular hydrogen. To better understand the electronic structure of phases containing these structural motifs, let us assume a full transfer of the metals' valence electrons to hydrogen, yielding H^- atoms, and $\text{H}_2^{\delta-}$ molecules. Phases with $\delta = 0$ are expected to metallize as a result of pressure induced broadening of the H^- and $\text{H}_2 \sigma^*$ anti-bonding based bands⁵¹. As a result, they generally do not have a high DOS at E_F , and they are therefore not expected to be good superconductors^{54,55}. Phases with $\delta > 0$, on the other hand, are metallic because of partial filling of the $\text{H}_2 \sigma^*$ -bands. As a result, they are likely to be good metals with the potential

for high temperature superconductivity.

One example of the former is the $I4/mmm$ symmetry CaH_4 (or $\text{Ca}^{2+}(\text{H}^-)_2\text{H}_2$) structure illustrated in Fig. 4(a), which was first predicted via CSP¹⁶⁷, and recently synthesized in a laser heated DAC¹⁴⁹. At 120 GPa a Bader analysis, which typically underestimates the charge transfer, yielded values of $\text{H}^{-0.5}$ and $\text{H}_2^{-0.05}$. The H-H bond length at 120 GPa, 0.81 Å, was found to be 33% larger than in H_2 at the same pressure. Theoretical calculations revealed that the weakening of the H-H bond in CaH_4 resembles the mechanism leading to anomalously long H-H bonds in Kubas-like molecular complexes wherein an H_2 molecule binds side-on to the metal center¹⁴⁹. In both the molecular and the high pressure systems donation of σ electrons from H_2 to a vacant metal d-orbital, and $d \rightarrow \sigma^*$ back-donation weaken the H-H bond. Because both the PBE-GGA and hybrid HSE06 functionals predicted that $I4/mmm$ CaH_4 would be a weak metal at this pressure, its T_c was not computed.

CSP calculations have also shown that isotopic SrH_4 ^{178,179} and MgH_4 ¹⁷³ phases are stable under pressure. Whereas $I4/mmm$ SrH_4 did not metallize within its range of stability, MgH_4 did, at least within PBE. Table II shows that the T_c of MgH_4 at 255 GPa was estimated to be close to the boiling point of liquid nitrogen. However, because this system metallizes as a result of pressure induced band broadening, PBE likely overestimates its DOS at E_F , and therefore its T_c . A BaH_4 stoichiometry did not lie on the convex hull¹⁸⁰.

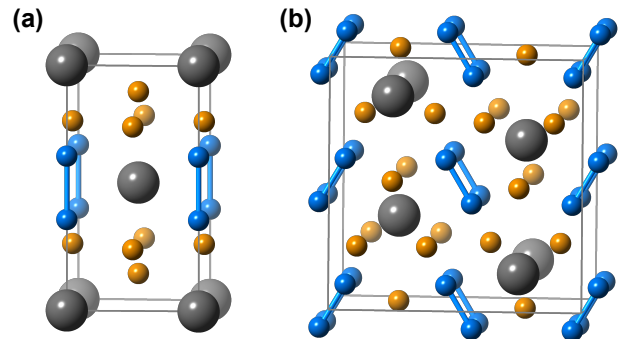


FIG. 4. (a) The $I4/mmm$ symmetry MH_4 structure that has been predicted to be stable for many of the alkaline earth and rare earth hydrides under pressure. (b) The crystal structure of $Cmc21$ ScH_7 at 300 GPa¹⁶⁹. Grey balls represent the metal atoms; white balls represent H^- atoms; $\text{H}_2^{\delta-}$ units are colored in blue.

DFT-based CSP searches have predicted that this same $I4/mmm$ symmetry structure will be stable for many of the rare earth metal tetrahydrides under pressure: ScH_4 ^{169-171,181}, YH_4 ¹⁷¹, LaH_4 ¹⁷⁴, CeH_4 ¹⁷¹ and PrH_4 ¹⁷¹. Moreover, theoretical studies that compared the enthalpies of a set of candidate structures, which were chosen based upon structural analogy, suggest that isotopic NdH_4 , PmH_4 , SmH_4 , EuH_4 , GdH_4 , TbH_4 , DyH_4 , HoH_4 , ErH_4 , TmH_4 , and LuH_4 phases lie on the convex hull at experimentally attainable pressures¹⁷¹. CSP searches also predicted that ZrH_4 would assume this

structure¹⁷³.

Out of all of the stable d -block $I4/mmm$ symmetry tetrahydrides, only ScH_4 and YH_4 were estimated to have T_c s above the boiling point of liquid nitrogen, see Table II. Assuming a +3 oxidation state for the metal atom yields a formula of $\text{M}^{3+}(\text{H}^-)_2\text{H}_2^-$ for these systems. Electron transfer into the H_2 σ^* -bands yields a high DOS at E_F , as expected. The nearest neighbor H-H distances measured 1.21 Å at 250 GPa in ScH_4 ¹⁶⁹, and 1.39 Å at 120 GPa in YH_4 ¹⁷². The long intramolecular H-H bond lengths, which are conducive to a large electron phonon coupling, have two origins. First, because these are d -elements the Kubas-like mechanism responsible for the elongation of the H_2 bond within $I4/mmm$ CaH_4 is likely to be important. Secondly, charge is donated from the electropositive element into the H_2 σ^* -bands, thereby weakening and lengthening the H-H bond.

An isotopic ZrH_4 phase was estimated to have a T_c of 47 K at 230 GPa¹⁷³. At this pressure the nearest neighbor H-H distance, 1.21 Å, and electron phonon coupling constant, $\lambda = 0.89$, was similar to the values computed for ScH_4 and YH_4 . The T_c of an $I4/mmm$ symmetry LaH_4 phase was estimated to be 5-10 K at 300 GPa¹⁷⁴. Its decreased T_c as compared to ScH_4 and YH_4 is likely a result of the lower frequency vibrations, which stem from the presence of the heavier metal atom. For similar reasons, the heavier $I4/mmm$ symmetry tetrahydrides are not expected to be superconducting at high temperatures, and their T_c s were therefore not computed¹⁷¹.

TABLE II. Electron phonon coupling parameter, λ , and superconducting critical temperature, T_c , of phases containing mixed molecular and atomic hydrogen computed at the pressures, P , and using the values of the Coulomb pseudopotential, μ^* , listed. Data is provided only for systems whose computed T_c s are higher than the boiling point of liquid nitrogen. MgH_4 , ScH_4 and YH_4 adopt the structure illustrated in Fig. 4(a). ScH_7 is shown in Fig. 4(b).

System	P (GPa)	λ	μ^*	T_c (K)
MgH_4	255	0.88	0.13	81 ^{b,173}
ScH_4	120	1.68	0.10	92 ^{a,169} , 163 ^{b,169}
	195	0.89	0.13-0.10	67-81 ^{a,170}
	200	0.99	0.10	98 ^{a,181}
YH_4	120	1.01	0.13-0.10	84-95 ^{b,172}
ScH_7	300	1.84	0.10	169 ^{a,169} , 213 ^{b,169}

^a T_c was calculated using the Allen-Dynes modified McMillan equation, Eq. 6.

^b T_c was calculated by solving the Eliashberg equations numerically.

Another phase with mixed molecular and atomic hydrogen that was predicted to be superconducting at high temperatures is the $Cmcm$ ScH_7 structure shown in Fig. 4(b)¹⁶⁹. Because this system contains three atomic and two molecular hydrogen atoms per scandium atom, at first glance one would guess that its chemical formula can be written as $\text{Sc}^{3+}(\text{H}^-)_3(\text{H}_2)_2$. At 300 GPa the H-H bond, which measures 0.956 Å, is significantly elongated relative to that of molecular H_2 at this pressure. In contrast to the results for CaH_4 , the computed average Bader charges on the “atomic” and “molecular” hy-

drogen atoms were nearly identical, $-0.186e$ and $-0.138e$, respectively, suggesting that the formula given above does not adequately describe the electronic structure of $Cmcm$ ScH_7 . Moreover, the substantial charge transfer to molecular hydrogen is consistent with its long H-H bond, the high DOS at E_F , and the large electron phonon coupling, which ultimately both yield a sizeable T_c .

C. Other Unique Hydrogenic Motifs

In addition to the aforementioned systems whose hydrogenic lattices were either clathrate-like or possessed molecular and atomic hydrogen, four more phases, with quite unusual hydrogenic motifs, were computed to be superconducting up to high temperatures. Comparison of Tables I and II with Table III reveals that their T_c values were generally intermediate to the other two classes of systems described above.

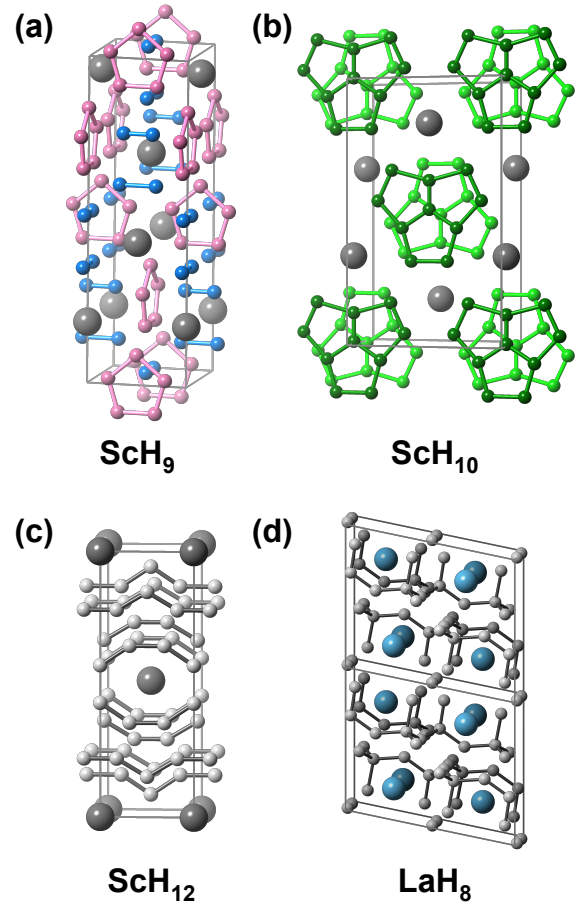


FIG. 5. The crystal structures of: (a) $I4_1md$ ScH_9 at 300 GPa, (b) $Cmcm$ ScH_{10} at 250 GPa and (c) $Immm$ ScH_{12} at 350 GPa¹⁶⁹. Grey balls represent the scandium atoms; white balls represent the hydrogen atoms; $\text{H}_5^{\delta-}$ units are colored in pink; $\text{H}_2^{\delta-}$ units are colored in blue; $\text{H}_{10}^{\delta-}$ units are colored in green.

$I4_1md$ ScH_9 , shown in Fig. 5(a), was predicted to be stable

in a narrow pressure range of 285-325 GPa when the ZPE was included¹⁶⁹. This phase contained 1-dimensional chains of edge-sharing $\text{H}_5^{\delta-}$ pentagons, as well as molecular $\text{H}_2^{\delta-}$ units, with the shortest H-H distance being 0.90 Å at 300 GPa. The hydrogenic lattice of a $Cmcm$ ScH_{10} phase^{169,171} consisted solely of these same “ H_5 ” pentagonal motifs, their edges shared so as to form discrete $\text{H}_{10}^{\delta-}$ molecular units, as illustrated in Fig. 5(b). One way to describe the hydrogenic lattice of the $Immm$ ScH_{12} structure shown in Fig. 5(c) would be of $\text{H}_8^{\delta-}$ “octagons” and $\text{H}_5^{\delta-}$ “pentagons”, where six edges of each octagon are connected by pentagons and the other edges opposite each other are connected by another octagon, thereby forming a 1-dimensional framework. The ZPE-corrected enthalpies at 0 K predicted that ScH_{10} and ScH_{12} would be thermodynamically stable between 220-285 GPa and above 325 GPa, respectively¹⁶⁹.

Finally, the LaH_8 stoichiometry was found to lie on the 150 GPa and 300 GPa convex hulls¹⁷⁴. At 300 GPa the 2-dimensional hydrogenic lattice of this $C2/c$ symmetry phase, shown in Fig. 5(d), consisted of edge-sharing puckered dodecagons wherein every second hydrogen atom was capped so that it became four-fold coordinate with H-H-H angles that deviated somewhat from those found in a perfect tetrahedron, 104.7°-116.3°. In addition, this phase contained hydrogen atoms, which did not appear to be bonded to any other hydrogen atoms, that fell between the puckered layers.

TABLE III. Electron phonon coupling parameter, λ , and superconducting critical temperature, T_c , of the $I4_1md$ ScH_9 , $Cmcm$ ScH_{10} , $Immm$ ScH_{12} , and $C2/m$ LaH_8 phases illustrated in Fig. 5, computed at the pressures, P , and using the values of the Coulomb pseudopotential, μ^* , provided.

System	P (GPa)	λ	μ^*	T_c (K)
$I4_1md$ ScH_9	300	1.94	0.10	163 ^{a,169} , 233 ^{b,169}
$Cmcm$ ScH_{10}	250	1.17	0.10	120 ^{a,169} , 143 ^{b,169}
$Immm$ ScH_{12}	350	1.23	0.10	141 ^{a,169} , 194 ^{b,169}
$C2/m$ LaH_8	300	1.12	0.13-0.10	114-131 ^{a,174} , 138-150 ^{b,174}

^a T_c was calculated using the Allen-Dynes modified McMillan equation, Eq. 6.

^b T_c was calculated by solving the Eliashberg equations numerically.

Even though a $P4/nmm$ BeH_2 phase was predicted to have a T_c of 97.0 K at 365 GPa, it is not discussed here since the hydrogen atoms within it were not bonded to each other¹⁸⁴. CSP searches showed that BeH_n with $n > 2$ are not thermodynamically stable with respect to decomposition into the classic BeH_2 hydride and H_2 up to 200 GPa¹⁸⁰. We also mention that an $Fddd$ symmetry ZrH_4 phase that was also only comprised of atomistic hydrogen (nearest neighbor H-H distance of 1.38 Å) was predicted to have a T_c of 78.0 K at 140 GPa¹⁷³. And that quite high T_c values, ranging from ~100-225 K, have also been predicted for some actinide polyhydrides with interesting structural motifs, for example $C2/m$ AcH_8 and $P6m2$ AcH_{16} , which become stable above ~100 GPa, or a metastable $I4/mmm$ AcH_{12} phase¹⁷⁶.

V. OUTLOOK

Crystal structure prediction techniques coupled with first-principles calculations have found a number of superconducting hydride phases that are either stable or metastable at pressures that can be achieved within diamond anvil cells. Binary hydrides with remarkably high estimated superconducting critical temperatures, T_c s, were predicted within two regions of the periodic table: the p -block elements and the alkaline earth and rare earths. Superconductivity up to 203 K was experimentally confirmed in the first region within a sample of hydrogen sulfide that was compressed to 150 GPa⁶⁵. This is the system with the record highest T_c confirmed to date. Recent experiments measuring T_c s of 215 K¹⁰³ or 260-280 K¹⁰⁴ in the lanthanum/hydrogen system under pressure suggest that the T_c of hydride phases in the second region may even surpass the record attributed to H_3S , and tempt with the lure of room temperature superconductivity.

Experimental techniques to synthesize high hydride phases under pressures have made remarkable advances in the last years⁶². We therefore expect the experimental search for superconductivity in these systems will accelerate, with the predictions from theory used as a guide. Given what has come before⁴¹, it is likely that a feedback loop between theory and experiment will be required to characterize the phases that have been made, and to gain an understanding of their electronic structure and properties.

The reason why hydrides with clathrate-based hydrogenic lattices are estimated to have such high T_c values can be traced back to their large density of states at the Fermi level, which is derived primarily from hydrogen-like states, and the pronounced impact on the electronic structure that results from the motions of the atoms comprising their hydrogenic lattices. It has been suggested that perturbing hydrogen atoms within quasi-molecular units such as $\text{H}_2^{\delta-}$ would not have such a large impact on the electronic structure, thereby resulting in a smaller electron-phonon coupling, with concomitantly lower T_c values^{55,56}. In accordance with this reasoning, the predicted T_c s for the MH_4 phases containing mixed molecular and atomic hydrogen are generally lower than those of the clathrate-like systems as shown in this Perspective.

However, this cannot be the full story because quite high T_c values have been calculated for a few of the scandium polyhydrides discussed herein whose hydrogenic lattices contain quasi-molecular units. Moreover, the factors driving the stability of these phases are not well understood, and it remains a grand challenge to find ways to quench these systems to pressures that can be easily achieved industrially. There is still much to be learned in this exciting field of research.

ACKNOWLEDGMENTS

We acknowledge the NSF (DMR-1505817) for financial, and the Center for Computational Research (CCR) at SUNY Buffalo for computational support. T. B. thanks the US Department of Energy, National Nuclear Security Administration, through the Capital-DOE Alliance Center under Coop-

erative Agreement DE-NA0003858 for financial support. We thank Prof. Yansun Yao from the University of Saskatchewan and Dr. Peng Feng from Luoyang Normal University for useful comments.

REFERENCES

- ¹E. Wigner and H. B. Huntington, *J. Chem. Phys.* **3**, 764 (1935).
- ²C. Narayana, H. Luo, J. Orloff, and A. L. Ruoff, *Nature* **393**, 46 (1998).
- ³P. Loubeyre, F. Occelli, and R. LeToullec, *Nature* **416**, 613 (2002).
- ⁴C. S. Zha, Z. Liu, M. Ahart, R. Boehler, and R. J. Hemley, *Phys. Rev. Lett.* **110**, 217402 (2013).
- ⁵M. I. Eremets and I. A. Troyan, *Nat. Mater.* **10**, 927 (2011).
- ⁶R. T. Howie, C. L. Guillaume, T. Scheler, A. F. Goncharov, and E. Gregoryanz, *Phys. Rev. Lett.* **108**, 125501 (2012).
- ⁷P. Dalladay-Simpson, R. T. Howie, and E. Gregoryanz, *Nature* **529**, 63 (2016).
- ⁸C. S. Zha, Z. Liu, and R. J. Hemley, *Phys. Rev. Lett.* **108**, 146402 (2012).
- ⁹R. T. Howie, T. Scheler, C. L. Guillaume, and E. Gregoryanz, *Phys. Rev. B* **86**, 214104 (2012).
- ¹⁰A. F. Goncharov, J. S. Tse, H. Wang, J. Yang, V. V. Struzhkin, R. T. Howie, and E. Gregoryanz, *Phys. Rev. B* **87**, 024101 (2013).
- ¹¹M. I. Eremets, I. A. Troyan, and A. P. Drozdov, arXiv:1601.04479 (2016).
- ¹²R. P. Dias and I. F. Silvera, *Science* **355**, 715 (2017).
- ¹³P. Loubeyre, F. Occelli, and P. Dumas, arXiv:1702.07192 (2017).
- ¹⁴M. I. Eremets and A. P. Drozdov, arXiv:1702.05125 (2017).
- ¹⁵X. D. Liu, P. Dalladay-Simpson, R. T. Howie, B. Li, and E. Gregoryanz, *Science* **357**, eaan2286 (2017).
- ¹⁶N. W. Ashcroft, *Phys. Rev. Lett.* **21**, 1748 (1968).
- ¹⁷P. Cudazzo, G. Profeta, A. Sanna, A. Floris, A. Continenza, S. Massidda, and E. K. U. Gross, *Phys. Rev. Lett.* **100**, 257001 (2008).
- ¹⁸J. M. McMahon and D. M. Ceperley, *Phys. Rev. B* **84**, 144515 (2011).
- ¹⁹N. W. Ashcroft, *Phys. Rev. Lett.* **92**, 187002 (2004).
- ²⁰N. W. Ashcroft, *J. Phys.: Condens. Matter* **16**, S945 (2004).
- ²¹J. Feng, W. Grochala, T. Jarof, R. Hoffmann, A. Bergara, and N. W. Ashcroft, *Phys. Rev. Lett.* **96**, 017006 (2006).
- ²²C. J. Pickard and R. J. Needs, *Phys. Rev. Lett.* **97**, 045504 (2006).
- ²³Y. Yao, J. S. Tse, Y. Ma, and K. Tanaka, *EPL* **78**, 37003 (2007).
- ²⁴O. Degtyareva, M. M. Canales, A. Bergara, X.-J. Chen, Y. Song, V. V. Struzhkin, H.-k. Mao, and R. J. Hemley, *Phys. Rev. B* **76**, 064123 (2007).
- ²⁵X.-J. Chen, J.-L. Wang, V. V. Struzhkin, H.-k. Mao, R. J. Hemley, and H.-Q. Lin, *Phys. Rev. Lett.* **101**, 077002 (2008).
- ²⁶D. Y. Kim, R. H. Scheicher, S. Lebègue, J. Prasongkit, B. Arnaud, M. Alouani, and R. Ahuja, *Proc. Natl. Acad. Sci. U.S.A.* **105**, 16454 (2008).
- ²⁷M. Martinez-Canales, A. R. Oganov, Y. Ma, Y. Yan, A. O. Lyakhov, and A. Bergara, *Phys. Rev. Lett.* **102**, 087005 (2009).
- ²⁸Y. Yan, J. Gong, and Z.-G. Zong, *Chin. Phys. Lett.* **27**, 017401 (2010).
- ²⁹H. Zhang, X. Jin, Y. Lv, Q. Zhuang, Y. Liu, Q. Lv, K. Bao, D. Li, B. Liu, and T. Cui, *Sci. Rep.* **5**, 8845 (2015).
- ³⁰W. Cui, J. Shi, H. Liu, Y. Yao, H. Wang, T. Iitaka, and Y. Ma, *Sci. Rep.* **5**, 13039 (2015).
- ³¹M. I. Eremets, I. A. Trojan, S. A. Medvedev, J. S. Tse, and Y. Yao, *Science* **319**, 1506 (2008).
- ³²M. Martinez-Canales, A. Bergara, J. Feng, and W. Grochala, *J. Phys. Chem. Solids* **67**, 2095 (2006).
- ³³Z. Li, W. Yu, and C. Jin, *Solid State Commun.* **143**, 353 (2007).
- ³⁴G. Gao, A. R. Oganov, A. Bergara, M. Martinez-Canales, T. Cui, T. Iitaka, Y. Ma, and G. Zou, *Phys. Rev. Lett.* **101**, 107002 (2008).
- ³⁵C. Zhang, X.-J. Chen, Y.-L. Li, V. V. Struzhkin, H.-K. Mao, R.-Q. Zhang, and H.-Q. Lin, *EPL* **90**, 66006 (2010).
- ³⁶H. Zhang, X. Jin, Y. Lv, Q. Zhuang, Q. Lv, Y. Liu, K. Bao, D. Li, B. Liu, and T. Cui, *Phys. Chem. Chem. Phys.* **17**, 27630 (2015).
- ³⁷C. J. Pickard and R. J. Needs, *Phys. Rev. B* **76**, 144114 (2007).
- ³⁸I. Goncharenko, M. I. Eremets, M. Hanfland, J. S. Tse, M. Amboage, Y. Yao, and I. A. Trojan, *Phys. Rev. Lett.* **100**, 045504 (2008).
- ³⁹D. Y. Kim, R. H. Scheicher, and R. Ahuja, *Phys. Rev. B* **78**, 100102(R) (2008).
- ⁴⁰M. Geshi and T. Fukazawa, *Physica B* **411**, 154 (2013).
- ⁴¹E. Zurek and W. Grochala, *Phys. Chem. Chem. Phys.* **17**, 2917 (2015).
- ⁴²E. Zurek, in *Handbook of Solid State Chemistry*, Vol. 5, edited by R. Dronskowski (Wiley-VCH Verlag GmbH & Co, 2017) pp. 571–605.
- ⁴³A. Hermann, in *Reviews in Computational Chemistry*, edited by A. L. Parrill and K. B. Lipkowitz (John Wiley & Sons, Inc., Hoboken, New Jersey, 2017) pp. 1–41.
- ⁴⁴T. A. Strobel, M. Somayazulu, and R. J. Hemley, *Phys. Rev. Lett.* **103**, 065701 (2009).
- ⁴⁵S. Wang, H.-k. Mao, X.-J. Chen, and W. L. Mao, *Proc. Natl. Acad. Sci. U.S.A.* **106**, 14763 (2009).
- ⁴⁶Y. Yao and D. D. Klug, *Proc. Natl. Acad. Sci. U.S.A.* **107**, 20893 (2010).
- ⁴⁷W.-L. Yim, J. S. Tse, and T. Iitaka, *Phys. Rev. Lett.* **105**, 215501 (2010).
- ⁴⁸K. Michel, Y. Liu, and V. Ozolins, *Phys. Rev. B* **82**, 174103 (2010).
- ⁴⁹K. V. Shanavas, H. K. Poswal, and S. M. Sharma, *Solid State Commun.* **152**, 873 (2012).
- ⁵⁰Y. Li, G. Gao, Y. Xie, Y. Ma, T. Cui, and G. Zou, *Proc. Natl. Acad. Sci. U.S.A.* **107**, 15708 (2010).
- ⁵¹E. Zurek, R. Hoffmann, N. W. Ashcroft, A. R. Oganov, and A. O. Lyakhov, *Proc. Natl. Acad. Sci. U.S.A.* **106**, 17640

- (2009).
- ⁵²C. Pépin, P. Loubeyre, F. Occelli, and P. Dumas, Proc. Natl. Acad. Sci. U.S.A. **112**, 7673 (2015).
- ⁵³The manuscripts where most of the T_c s were obtained are either referenced in this manuscript or in Ref.⁶², with the exception of Ref.¹⁸⁵ (AtH_n) and Ref.¹⁸⁶ (ArH_n).
- ⁵⁴E. Zurek, Comments Inorg. Chem. **37**, 78 (2017).
- ⁵⁵A. Shamp and E. Zurek, Nov. Supercond. Mater. **3**, 14 (2017).
- ⁵⁶L. Zhang, Y. Wang, J. Lv, and Y. Ma, Nature Rev. Mater. **2**, 17005 (2017).
- ⁵⁷D. Duan, Y. Liu, Y. Ma, Z. Shao, B. Liu, and T. Cui, Natl. Sci. Rev. **4**, 121 (2016).
- ⁵⁸H. Wang, X. Li, G. Gao, Y. Li, and Y. Ma, Wiley Interdiscip. Rev. Comput. Mol. Sci. **8**, 1 (2017).
- ⁵⁹V. V. Struzhkin, Physica C **514**, 77 (2015).
- ⁶⁰R. J. Needs and C. J. Pickard, APL Mater. **4**, 053210 (2016).
- ⁶¹Y. Yao and J. S. Tse, Chem. Eur. J **24**, 1769 (2018).
- ⁶²T. Bi, N. Zarifi, T. Terpstra, and E. Zurek, arXiv:1806.00163 (2018).
- ⁶³D. V. Semenov, I. A. Kruglov, A. G. Kvashnin, and A. R. Oganov, arXiv:1806.00865 (2018).
- ⁶⁴The high T_c values predicted for FeH₅^{187,188} are not included, since subsequent studies^{151,189} have questioned these results.
- ⁶⁵A. P. Drozdov, M. I. Eremets, I. A. Troyan, V. Ksenofontov, and S. I. Shylin, Nature **525**, 73 (2015).
- ⁶⁶I. I. Mazin, Nature **525**, 40 (2015).
- ⁶⁷Y. Li, J. Hao, H. Liu, Y. Li, and Y. Ma, J. Chem. Phys. **140**, 174712 (2014).
- ⁶⁸D. Duan, Y. Liu, F. Tian, D. Li, X. Huang, Z. Zhao, H. Yu, B. Liu, W. Tian, and T. Cui, Sci. Rep. **4**, 6968 (2014).
- ⁶⁹M. Einaga, M. Sakata, T. Ishikawa, K. Shimizu, M. I. Eremets, A. P. Drozdov, I. A. Troyan, N. Hirao, and Y. Ohishi, Nat. Phys. **12**, 835 (2016).
- ⁷⁰I. Troyan, A. Gavriluk, R. Rüffer, A. Chumakov, A. Mironovich, I. Lyubutin, D. Perekalin, A. P. Drozdov, and M. I. Eremets, Science **351**, 1303 (2016).
- ⁷¹F. Capitani, B. Langerome, J. B. Brubach, P. Roy, A. Drozdov, M. I. Eremets, E. J. Nicol, J. P. Carbotte, and T. Timusk, Nat. Phys. **13**, 859 (2017).
- ⁷²A. F. Goncharov, S. S. Lobanov, V. B. Prakapenka, and E. Greenberg, Phys. Rev. B **95**, 140101(R) (2017).
- ⁷³B. Guigue, A. Marizy, and P. Loubeyre, Phys. Rev. B **95**, 020104(R) (2017).
- ⁷⁴J. A. Flores-Livas, A. Sanna, and E. K. U. Gross, Eur. Phys. J. B. **89**, 1 (2016).
- ⁷⁵D. A. Papaconstantopoulos, B. M. Klein, M. J. Mehl, and W. E. Pickett, Phys. Rev. B **91**, 184511 (2015).
- ⁷⁶N. Bernstein, C. S. Hellberg, M. D. Johannes, I. I. Mazin, and M. J. Mehl, Phys. Rev. B **91**, 060511(R) (2015).
- ⁷⁷D. Duan, X. Huang, F. Tian, D. Li, H. Yu, Y. Liu, Y. Ma, B. Liu, and T. Cui, Phys. Rev. B **91**, 180502(R) (2015).
- ⁷⁸I. Errea, M. Calandra, C. J. Pickard, J. Nelson, R. J. Needs, Y. Li, H. Liu, Y. Zhang, Y. Ma, and F. Mauri, Phys. Rev. Lett. **114**, 157004 (2015).
- ⁷⁹R. Akashi, M. Kawamura, S. Tsuneyuki, Y. Nomura, and R. Arita, Phys. Rev. B **91**, 224513 (2015).
- ⁸⁰I. Errea, M. Calandra, C. J. Pickard, J. R. Nelson, R. J. Needs, Y. Li, H. Liu, Y. Zhang, Y. Ma, and F. Mauri, Nature **532**, 81 (2016).
- ⁸¹Y. Quan and W. E. Pickett, Phys. Rev. B **93**, 104526 (2016).
- ⁸²W. Sano, T. Koretsune, T. Tadano, R. Akashi, and R. Arita, Phys. Rev. B **93**, 094525 (2016).
- ⁸³L. Ortenzi, E. Cappelluti, and L. Pietronero, Phys. Rev. B **94**, 064507 (2016).
- ⁸⁴L. P. Gor'kov and V. Z. Kresin, Sci. Rep. **6**, 25608 (2016).
- ⁸⁵A. F. Goncharov, S. S. Lobanov, I. Kruglov, X. M. Zhao, X. J. Chen, A. R. Oganov, Z. Konôpková, and V. B. Prakapenka, Phys. Rev. B **93**, 174105 (2016).
- ⁸⁶A. Bussmann-Holder, J. Köhler, A. Simon, M. Whangbo, and A. Bianconi, J. Supercond. Nov. Magn. **30**, 151 (2017).
- ⁸⁷A. P. Durajski, Sci. Rep. **6**, 38570 (2016).
- ⁸⁸T. Jarlborg and A. Bianconi, Sci. Rep. **6**, 24816 (2016).
- ⁸⁹R. Szcześniak and A. P. Durajski, Solid State Commun. **249**, 30 (2017).
- ⁹⁰S. Azadi and T. D. Kühne, J. Chem. Phys. **146**, 084503 (2017).
- ⁹¹A. P. Durajski, R. Szcześniak, and Y. Li, Physica C **515**, 1 (2015).
- ⁹²R. Arita, T. Koretsune, S. Sakai, R. Akashi, Y. Nomura, and W. Sano, Adv. Mater. **29**, 1602421 (2017).
- ⁹³E. E. Gordon, K. Xu, H. Xiang, A. Bussmann-Holder, R. K. Kremer, A. Simon, J. Köhler, and M. H. Whangbo, Angew. Chem. Int. Ed. **55**, 3682 (2016).
- ⁹⁴A. Majumdar, J. S. Tse, and Y. Yao, Angew. Chem. Int. Ed. **56**, 11390 (2017).
- ⁹⁵R. Akashi, W. Sano, R. Arita, and S. Tsuneyuki, Phys. Rev. Lett. **117**, 075503 (2016).
- ⁹⁶Y. Li, L. Wang, H. Liu, Y. Zhang, J. Hao, C. J. Pickard, J. R. Nelson, R. J. Needs, W. Li, Y. Huang, I. Errea, M. Calandra, F. Mauri, and Y. Ma, Phys. Rev. B **93**, 020103(R) (2016).
- ⁹⁷T. Ishikawa, A. Nakanishi, K. Shimizu, H. Katayama-Yoshida, T. Oda, and N. Suzuki, Sci. Rep. **6**, 23160 (2016).
- ⁹⁸C. Heil and L. Boeri, Phys. Rev. B **92**, 060508(R) (2015).
- ⁹⁹Y. Ge, F. Zhang, and Y. Yao, Phys. Rev. B **93**, 224513 (2016).
- ¹⁰⁰A. Bianconi and T. Jarlborg, EPL **112**, 37001 (2015).
- ¹⁰¹M. I. Eremets and A. P. Drozdov, Phys. -Usp. **59**, 1154 (2016).
- ¹⁰²M. Einaga, M. Sakata, A. Masuda, K. Shimizu, A. Drozdov, M. Eremets, S. Kawaguchi, N. Hirao, and Y. Ohishi, Jpn. J. Appl. Phys. **56**, 05FA13 (2017).
- ¹⁰³A. P. Drozdov, V. S. Minkov, S. P. Besedin, P. P. Kong, M. A. Kuzovnikov, D. A. Knyazev, and M. I. Eremets, arXiv:1808.07039 (2018).
- ¹⁰⁴M. Somayazulu, M. Ahart, A. K. Mishra, Z. M. Geballe, M. Baldini, Y. Meng, V. V. Struzhkin, and R. J. Hemley, arXiv:1808.07695 (2018).
- ¹⁰⁵R. J. Hemley, Annu. Rev. Phys. Chem. **51**, 763 (2000).
- ¹⁰⁶Y. Song, Phys. Chem. Chem. Phys. **15**, 14524 (2013).
- ¹⁰⁷W. Grochala, R. Hoffmann, J. Feng, and N. W. Ashcroft, Angew. Chem. Int. Ed. **46**, 3620 (2007).

- ¹⁰⁸A. F. Goncharov, R. T. Howie, and E. Gregoryanz, *Low Temp. Phys.* **39**, 402 (2013).
- ¹⁰⁹P. Bhardwaj and S. Singh, *Cent. Eur. J. Chem.* **10**, 1391 (2012).
- ¹¹⁰L. Dubrovinsky and N. Dubrovinskaia, in *Comprehensive Inorganic Chemistry II (Second Edition): From Elements to Applications*, Vol. 2 (Elsevier, 2013) pp. 223–239.
- ¹¹¹P. F. McMillan, in *Comprehensive Inorganic Chemistry II (Second Edition): From Elements to Applications*, Vol. 2 (Elsevier, 2013) pp. 17–46.
- ¹¹²D. D. Klug and Y. Yao, *Phys. Chem. Chem. Phys.* **13**, 16999 (2011).
- ¹¹³I. I. Naumov and R. J. Hemley, *Acc. Chem. Res.* **47**, 3551 (2014).
- ¹¹⁴Y. Ma, M. Eremets, A. R. Oganov, Y. Xie, I. Trojan, S. Medvedev, A. O. Lyakhov, M. Valle, and V. Prakapenka, *Nature* **458**, 182 (2009).
- ¹¹⁵X. Dong, A. R. Oganov, A. F. Goncharov, E. Stavrou, S. Lobanov, G. Saleh, G. R. Qian, Q. Zhu, C. Gatti, V. L. Deringer, R. Dronskowski, X. F. Zhou, V. B. Prakapenka, Z. Konopkova, I. A. Popov, A. I. Boldyrev, and H. T. Wang, *Nat. Chem.* **9**, 440 (2017).
- ¹¹⁶Z. Liu, J. Botana, A. Hermann, E. Zurek, D. Yan, H. Lin, and M. Miao, *Nat. Commun.* **9**, 951 (2018).
- ¹¹⁷V. V. Struzhkin, D. Y. Kim, E. Stavrou, T. Muramatsu, H. k. Mao, C. J. Pickard, R. J. Needs, V. B. Prakapenka, and A. F. Goncharov, *Nat. Commun.* **7**, 12267 (2016).
- ¹¹⁸M. Somayazulu, P. Dera, A. F. Goncharov, S. A. Gramsch, P. Liermann, W. Yang, Z. Liu, H. K. Mao, and R. J. Hemley, *Nat. Chem.* **2**, 50 (2010).
- ¹¹⁹C. M. Pépin, G. Geneste, A. Dewaele, M. Mezouar, and P. Loubeyre, *Science* **357**, 382 (2017).
- ¹²⁰S. M. Woodley and R. Catlow, *Nat. Mater.* **7**, 937 (2008).
- ¹²¹J. C. Schön, K. Doll, and M. Jansen, *Phys. Status Solidi B* **247**, 23 (2010).
- ¹²²G. Rossi and R. Ferrando, *J. Phys.: Condens. Matter* **21**, 084208 (2009).
- ¹²³Y. Wang and Y. Ma, *J. Chem. Phys.* **140**, 040901 (2014).
- ¹²⁴C. J. Pickard and R. J. Needs, *Phys. Status Solidi B* **246**, 536 (2009).
- ¹²⁵B. C. Revard, W. W. Tipton, and R. G. Hennig (Springer Berlin Heidelberg, 2014) pp. 181–222.
- ¹²⁶A. R. Oganov, ed., *Modern Methods of Crystal Structure Prediction* (Wiley-VCH, 2011).
- ¹²⁷D. J. Wales, *Energy Landscapes: Applications to Clusters, Biomolecules and Glasses* (Cambridge: Cambridge University Press, 2003).
- ¹²⁸E. Zurek, in *Reviews in Computational Chemistry*, Vol. 29, edited by A. L. Parrill and K. B. Lipkowitz (John Wiley & Sons, Inc., Hoboken, New Jersey, 2016) pp. 274–326.
- ¹²⁹A. R. Oganov, A. O. Lyakhov, and M. Valle, *Acc. Chem. Res.* **44**, 227 (2011).
- ¹³⁰M. Jansen, *Adv. Mater.* **27**, 3229 (2015).
- ¹³¹J. P. Perdew, K. Burke, and M. Ernzerhof, *Phys. Rev. Lett.* **77**, 3865 (1996).
- ¹³²A. V. Krukau, O. A. Vydrov, A. F. Izmaylov, and G. E. Scuseria, *J. Chem. Phys.* **125**, 224106 (2006).
- ¹³³C. Adamo and V. Barone, *J. Chem. Phys.* **110**, 6158 (1999).
- ¹³⁴H. Liu, W. Cui, and Y. Ma, *J. Chem. Phys.* **137**, 184502 (2012).
- ¹³⁵A. M. Teweldeberhan, J. L. DuBois, and S. A. Bonev, *Phys. Rev. B* **86**, 064104 (2012).
- ¹³⁶A. J. Ochoa-Calle, C. M. Zicovich-Wilson, and A. Ramirez-Solis, *Phys. Rev. B* **92**, 085148 (2015).
- ¹³⁷D. Kurzydłowski and P. Zaleski-Ejgierd, *Phys. Chem. Chem. Phys.* **18**, 2309 (2016).
- ¹³⁸D. Kurzydłowski and P. Zaleski-Ejgierd, *Sci. Rep.* **6**, 36049 (2016).
- ¹³⁹A. Hermann, M. Derzsi, W. Grochala, and R. Hoffmann, *Inorg. Chem.* **55**, 1278 (2016).
- ¹⁴⁰M. Komelj and H. Krakauer, *Phys. Rev. B* **92**, 205125 (2015).
- ¹⁴¹B. Boates and S. A. Bonev, *Phys. Rev. B* **83**, 174114 (2011).
- ¹⁴²B. Santra, J. Klimeš, D. Alfè, A. Tkatchenko, B. Slater, A. Michaelides, R. Car, and M. Scheffler, *Phys. Rev. Lett.* **107**, 185701 (2011).
- ¹⁴³B. Santra, J. Klimeš, A. Tkatchenko, D. Alfè, B. Slater, A. Michaelides, R. Car, and M. Scheffler, *J. Chem. Phys.* **139**, 154702 (2013).
- ¹⁴⁴D. Kurzydłowski, *Crystals* **8**, 140 (2018).
- ¹⁴⁵S. Q. Wu, M. Ji, C. Z. Wang, M. C. Nguyen, X. Zhao, K. Umamoto, R. M. Wentzcovitch, and K. M. Ho, *J. Phys.: Condens. Matter* **26**, 035402 (2014).
- ¹⁴⁶J. Hooper and E. Zurek, *Chem. Eur. J.* **18**, 5013 (2012).
- ¹⁴⁷P. Zaleski-Ejgierd, R. Hoffmann, and N. W. Ashcroft, *Phys. Rev. Lett.* **107**, 037002 (2011).
- ¹⁴⁸C. J. Pickard, M. Martinez-Canales, and R. J. Needs, *Phys. Rev. B* **85**, 214114 (2012).
- ¹⁴⁹A. K. Mishra, T. Muramatsu, H. Liu, Z. M. Geballe, M. Somayazulu, M. Ahart, M. Baldini, Y. Meng, E. Zurek, and R. J. Hemley, *J. Phys. Chem. C* **122**, 19370 (2018).
- ¹⁵⁰A. P. Drozdov, M. I. Eremets, and I. A. Troyan, *arXiv:1508.06224* (2015).
- ¹⁵¹N. Zarifi, T. Bi, H. Liu, and E. Zurek, *J. Phys. Chem. C* **122**, 24262 (2018).
- ¹⁵²Y. Wang, J. Lv, L. Zhu, and Y. Ma, *Phys. Rev. B* **82**, 094116 (2010).
- ¹⁵³Y. Wang, J. Lv, L. Zhu, and Y. Ma, *Comput. Phys. Commun.* **183**, 2063 (2012).
- ¹⁵⁴C. W. Glass, A. R. Oganov, and N. Hansen, *Comput. Phys. Commun.* **175**, 713 (2006).
- ¹⁵⁵D. C. Lonie and E. Zurek, *Comput. Phys. Commun.* **182**, 372 (2011).
- ¹⁵⁶C. J. Pickard and R. J. Needs, *J. Phys.: Condens. Matter* **23**, 053201 (2011).
- ¹⁵⁷S. K. Bose and J. Kortus, in *Vibronic and Electron-Phonon Interactions and Their Role in Modern Chemistry and Physics*, edited by T. Kato (Transworld Research Network, Kerala, India, 2009) pp. 1–62.
- ¹⁵⁸J. Bardeen, L. N. Cooper, and J. R. Schrieffer, *Phys. Rev.* **106**, 162 (1957).
- ¹⁵⁹J. Bardeen, L. N. Cooper, and J. R. Schrieffer, *Phys. Rev.* **108**, 1175 (1957).
- ¹⁶⁰G. M. Eliashberg, *Sov. Phys. JETP* **11**, 696 (1960).

- ¹⁶¹M. Lüders, M. A. L. Marques, N. N. Lathiotakis, A. Floris, G. Profeta, L. Fast, A. Continenza, S. Massidda, and E. K. U. Gross, *Phys. Rev. B* **72**, 024545 (2005).
- ¹⁶²M. A. L. Marques, M. Lüders, N. N. Lathiotakis, G. Profeta, A. Floris, L. Fast, A. Continenza, E. K. U. Gross, and S. Massidda, *Phys. Rev. B* **72**, 024546 (2005).
- ¹⁶³J. A. Flores-Livas, M. Amsler, C. Heil, A. Sanna, L. Boeri, G. Profeta, C. Wolverton, S. Goedecker, and E. K. U. Gross, *Phys. Rev. B* **93**, 020508(R) (2016).
- ¹⁶⁴W. L. McMillan, *Phys. Rev.* **167**, 331 (1968).
- ¹⁶⁵P. B. Allen and R. C. Dynes, *Phys. Rev. B* **12**, 905 (1975).
- ¹⁶⁶R. C. Dynes, *Solid State Commun.* **10**, 615 (1972).
- ¹⁶⁷H. Wang, J. S. Tse, K. Tanaka, T. Iitaka, and Y. Ma, *Proc. Natl. Acad. Sci. U.S.A.* **109**, 6463 (2012).
- ¹⁶⁸X. Feng, J. Zhang, G. Gao, H. Liu, and H. Wang, *RSC Adv.* **5**, 59292 (2015).
- ¹⁶⁹X. Ye, N. Zarifi, E. Zurek, R. Hoffmann, and N. W. Ashcroft, *J. Phys. Chem. C* **122**, 6298 (2018).
- ¹⁷⁰K. Abe, *Phys. Rev. B* **96**, 144108 (2017).
- ¹⁷¹F. Peng, Y. Sun, C. J. Pickard, R. J. Needs, Q. Wu, and Y. Ma, *Phys. Rev. Lett.* **119**, 107001 (2017).
- ¹⁷²Y. Li, J. Hao, H. Liu, J. S. Tse, Y. Wang, and Y. Ma, *Sci. Rep.* **5**, 9948 (2015).
- ¹⁷³K. Abe, *Phys. Rev. B* **98**, 134103 (2018).
- ¹⁷⁴H. Liu, I. I. Naumov, R. Hoffmann, N. W. Ashcroft, and R. J. Hemley, *Proc. Natl. Acad. Sci. U.S.A.* **114**, 6990 (2017).
- ¹⁷⁵H. Liu, I. I. Naumov, Z. M. Geballe, M. Somayazulu, J. S. Tse, and R. J. Hemley, *Phys. Rev. B* **98**, 100102(R) (2018).
- ¹⁷⁶D. V. Semenov, A. G. Kvashnin, I. A. Kruglov, and A. R. Oganov, *J. Phys. Chem. Lett.* **9**, 1920 (2018).
- ¹⁷⁷D. C. Lonie, J. Hooper, B. Altintas, and E. Zurek, *Phys. Rev. B* **87**, 054107 (2013).
- ¹⁷⁸J. Hooper, T. Terpstra, A. Shamp, and E. Zurek, *J. Phys. Chem. C* **118**, 6433 (2014).
- ¹⁷⁹Y. Wang, H. Wang, J. S. Tse, T. Iitaka, and Y. Ma, *Phys. Chem. Chem. Phys.* **17**, 19379 (2015).
- ¹⁸⁰J. Hooper, B. Altintas, A. Shamp, and E. Zurek, *J. Phys. Chem. C* **117**, 2982 (2013).
- ¹⁸¹S. Qian, X. Sheng, X. Yan, Y. Chen, and B. Song, *Phys. Rev. B* **96**, 094513 (2017).
- ¹⁸²M. Amri, G. J. Clarkson, and R. I. Walton, *J. Phys. Chem. C* **114**, 6726 (2010).
- ¹⁸³Z. M. Geballe, H. Liu, A. K. Mishra, M. Ahart, M. Somayazulu, Y. Meng, M. Baldini, and R. J. Hemley, *Angew. Chem. Int. Ed.* **57**, 688 (2018).
- ¹⁸⁴S. Yu, Q. Zeng, A. R. Oganov, C. Hu, G. Frapper, and L. Zhang, *AIP Adv.* **4**, 107118 (2014).
- ¹⁸⁵Z. Shao, Y. Huang, D. Duan, Y. Ma, H. Yu, H. Xie, D. Li, F. Tian, B. Liu, and T. Cui, *Phys. Chem. Chem. Phys.* **20**, 24783 (2018).
- ¹⁸⁶T. Ishikawa, A. Nakanishi, K. Shimizu, and T. Oda, *J. Phys. Soc. Jpn.* **86**, 124711 (2017).
- ¹⁸⁷A. Majumdar, J. S. Tse, M. Wu, and Y. Yao, *Phys. Rev. B* **96**, 201107(R) (2017).
- ¹⁸⁸A. G. Kvashnin, I. A. Kruglov, D. V. Semenov, and A. R. Oganov, *J. Phys. Chem. C* **122**, 4731 (2018).
- ¹⁸⁹C. Heil, G. B. Bachelet, and L. Boeri, *Phys. Rev. B* **97**, 214510 (2018).